Nuclear Instruments and Methods in Physics Research A 678 (2012) 83–87

Contents lists available at SciVerse ScienceDirect

Nuclear Instruments and Methods in Physics Research A

journal homepage: www.elsevier.com/locate/nima

High rate read-out of LaBr(Ce) scintillator with a fast digitizer

L. Stevanato [a,*], D. Cester [a], G. Nebbia [b], G. Viesti [a], F. Neri [c], S. Petrucci [c], S. Selmi [c], C Tintori [c]

[a] Dipartimento di Fisica ed Astronomia, Università di Padova, Via Marzolo 8, I-35131 Padova, Italy
[b] INFN Sezione di Padova, Via Marzolo 8, I-35131 Padova, Italy
[c] CAEN S.p.A., Via Vetraia 11, I-55049 Viareggio (LU), Italy

ARTICLE INFO

Article history:
Received 17 November 2011
Received in revised form
29 February 2012
Accepted 4 March 2012
Available online 23 March 2012

Keywords:
LaBr(Ce) scintillator
Digital signal processing

ABSTRACT

The energy resolution of a LaBr(Ce) detector has been studied as a function of the count rate up to 340 kHz by using a 12 bit 250 MS/s V1720 digitizer. The time resolution achieved by processing off line the digitized signals has been also determined. It appears that the energy resolution obtained with the digitizer is better than that achievable using standard NIM electronics. The time resolution yielded by the digitizer with a software CFTD is about $\delta t = 0.8$ ns (FWHM), slightly worse with respect to $\delta t = 0.65$ ns (FWHM) obtained from standard NIM. However, this time resolution lies well within the requirements for applications in Non-Destructive Analysis of large objects with tagged neutron beams.

1. Introduction

The Sistema Mobile per Analisi Non Distruttive e RAdiometriche (SMANDRA) mobile inspection system [1] has been designed within the SLIMPORT project [2] to detect and identify threat or dangerous materials including sources of ionizing radiation and special nuclear material (SNM) as well as explosives and/or illegal materials inside volumes tagged as "suspect" by conventional X-ray scanners. The SMANDRA detector unit includes gamma-ray and neutron detectors and can be used in standalone mode as a spectroscopic radiometer as well as detector package connected to a neutron generator for active interrogation using the Tagged Neutron Inspection System (TNIS) technique [3].

The dual use of SMANDRA (in active and passive interrogations) sets stringent requirements. In passive interrogations the system has to be equipped with low background, high efficiency detectors for gamma and neutrons, giving the capability to discriminate the gamma-ray from the neutron component of the radiation. In active interrogation making use of tagged 14 MeV neutrons it is mandatory to have detectors with good time resolution and high count rate capability.

In the SMANDRA system the front end electronics is based on a VME CAEN-V1720 digitizer used to perform digital pulse processing by FPGA.

In this paper results are reported on laboratory tests aimed at studying the capability of this VME front end in connection with a LaBr(Ce) scintillator. Comparison with traditional NIM based electronics is as well presented.

2. Experimental details

The SMANDRA system includes a 2 in. × 2 in. BrilLanCe™ 380 LaBr(Ce) detector from Saint-Gobain equipped with a standard R6231-1 photomultiplier with AS20 voltage divider. The LaBr(Ce) scintillator exhibits some remarkable properties that make it interesting in basic science as well as in several applications (homeland security, medical imaging, geophysical sciences) thanks to its superior energy resolution and fast response (see as example [4]).

It is worth mentioning that the R6231 PMTs have been often used with LaBr(Ce) crystals in spectroscopic applications thanks to their high photocathode quantum efficiency and it represents today a reference PMT for such applications [5,6]. However this type of PMT is a relatively slow device with a large transit time spread not properly suited for optimal fast timing applications.

The front end electronics is based on a prototype battery operated VME mini-crate (4 slots) with a Bridge USB V1718. The mini-crate hosts an HV system V6533 Programmable HV Power Supply (6 Ch., 4 kV, 3 mA, 9 W) and a V1720 8 Channel 12 bit 250 MS/s Digitizer [7].

Inside the V1720 card, Digital Pulse Processing (DPP) algorithms are implemented by using FPGA, providing on-line for each event (a) a time stamp, (b) a complete integration of the signal, and (c) the possibility of storing a selected part of the digitized signal.

In the V1720 card some parameters need to be tuned in order to optimize the achievable energy resolution from the digital pulse

* Corresponding author. Tel.: +390 49 8275936; fax: +390 49 8275961.
E-mail address: luca.stevanato@pd.infn.it (L. Stevanato).

0168-9002/$ - see front matter © 2012 Elsevier B.V. All rights reserved.
http://dx.doi.org/10.1016/j.nima.2012.03.016

processing performed by FPGA. A detailed description of the DPP algorithm can be found in Ref. [8], including a detailed sketch on how the digital pulse processing parameters work. The DPP parameters relevant for the present application are the Gate Width i.e. the number of FADC bins used in the energy integration, the Gate Pre Trigger Width that establishes the number of bins before the crossing of the low energy threshold from which the signal integration is started and the baseline mean i.e. the number of bins used for the definition of the baseline level. Such optimization was performed empirically by scanning over a range of possible values of the three parameters and measuring for each setting the energy resolution $\delta E/E$, calculated as FWHM/E, at $E\gamma=1274$ keV with a ^{22}Na source. As an example, the results obtained in optimizing the DPP parameters are reported in Table 1. The optimization was operated sequentially by changing one parameter at a time in a iterative way. The reported data refers to the final fine tuning. The digitizer bins are 4 ns wide.

The radioactive gamma ray sources available in our laboratory have a typical activity of 400 kBq each. Variable detector rate is obtained by changing the source–detector distance and/or grouping several sources together.

3. Energy resolution results

The energy resolution of the LaBr(Ce) scintillator was first tested up to about 20 kHz by using standard NIM electronics (ORTEC Amplifier mod.570) and a ^{22}Na source. The measured energy resolution $\delta E/E$, is rather constant with the rate by using Shaping Time values ST=0.5 or 1.0 μs. Typical values are $\delta E/E=3.7\%$ at 551 keV and $\delta E/E=2.25\%$ at 1275 keV, in agreement with the factory specification (in our case energy resolution lower than 3.5% at 662 keV). Our measured energy resolutions are comparable with those reported in Refs. [9,10] for 2 in. × 2 in. and 3 in. × 3 in. crystals with standard NIM electronics read-out.

Then a number of measurements were performed using the V1720 digitizer with the optimized DPP parameters. A sample of the spectra obtained at two different rates is reported in Fig. 1.

In Fig. 2 summary of the energy resolution measured as a function of count rate is presented. The energy resolution is generally better than that measured using standard NIM electronics, and is generally also better than the value declared by Saint-Gobain up to very high rates, i.e. 340 kHz. However a degradation of the energy resolution is evidenced for detector rates larger than about 100 kHz.

To better understand the energy resolution behavior, a specific test of the V1720 card was performed by using a BNC Pulse Generator mod. PB-4 and a Timing Filter Amplifier ORTEC mod. 474 to obtain pulses with a shape similar to the LaBr(Ce). Results from the pulser test, reported in Fig. 3, show that the electronics contribution to energy resolution is in the range $\delta E/E=0.50\pm 0.05\%$ up to about 180 kHz and then increases up to about $\delta E/E=0.6\%$ at 220 kHz. Such contribution to the overall energy resolution reported in Fig. 2 is certainly negligible and its variation with the rate does not explain the registered worsening of the overall energy resolution.

It is worth mentioning that very high count rate applications of LaBr(Ce) scintillators have been recently reported in the field of safeguards [11] and plasma diagnostics [12]. Although a direct comparison of our measured energy resolution at high rate is not possible, it is interesting to note that in Ref. 11the reported energy resolution is lower than $\delta E/E=2.4\%$ at 662 keV for a 1.5 in. × 1.5 in. crystal up to 40 kHz.

Table 1
Example of the V1720 DPP parameter optimization.

Parameter	Range explored (bins)	Energy resolution $\delta E/E$, min–max (%)	Optimum value (bins)
Baseline mean	3–10	2.15–2.17	5
Gate Pre-trigger width	6–12	2.15–2.39	8
Gate width	25–60	2.12–2.24	40

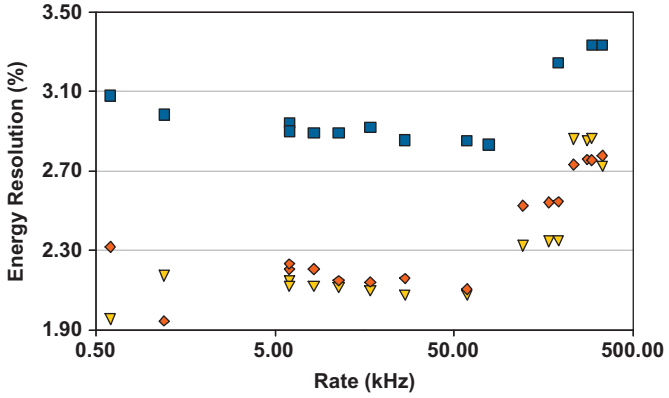

Fig. 2. Measured energy resolution of the LaBr(Ce) scintillator with the V1720 read-out as a function of the count rate. Squares are relative to the ^{137}Cs gamma line (0.662 MeV) whereas triangles and diamonds are related to the ^{60}Co lines (1.33 and 1.17 MeV).

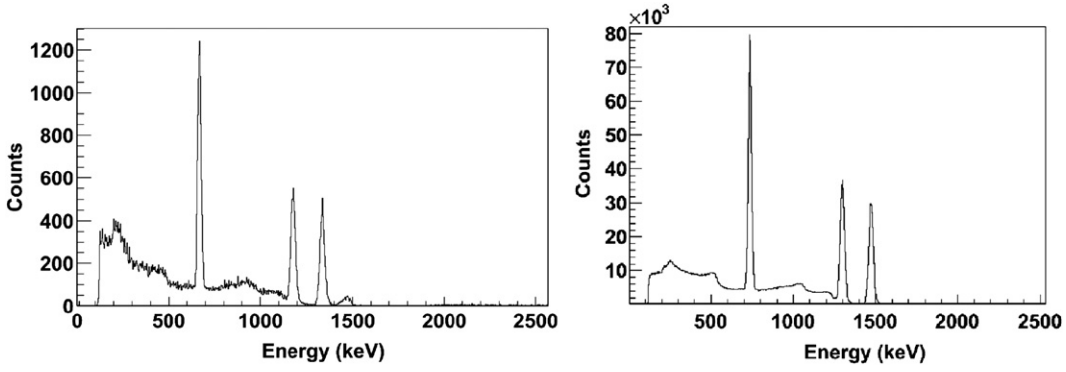

Fig. 1. Gamma ray spectra measured with the LaBr(Ce) scintillator with a ^{137}Cs and a ^{60}Co source at total rate of 1.5 kHz (left panel) and 145 kHz (right panel). The energy calibration was established at the lower rate. For details see the text.

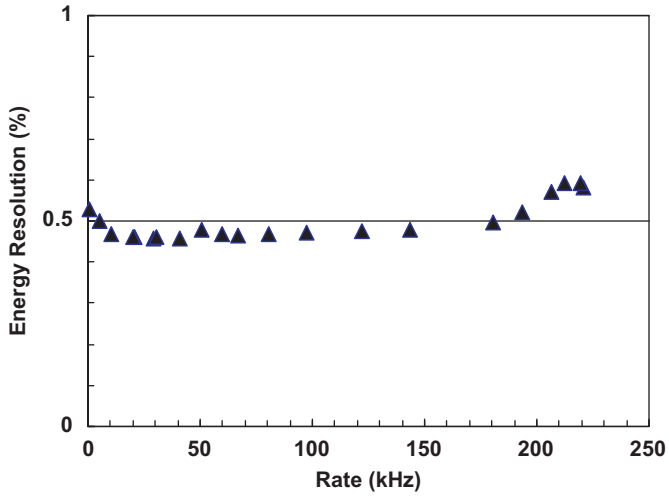

Fig. 3. Energy resolution of the V1720 card as a function of the rate measured during the pulser tests.

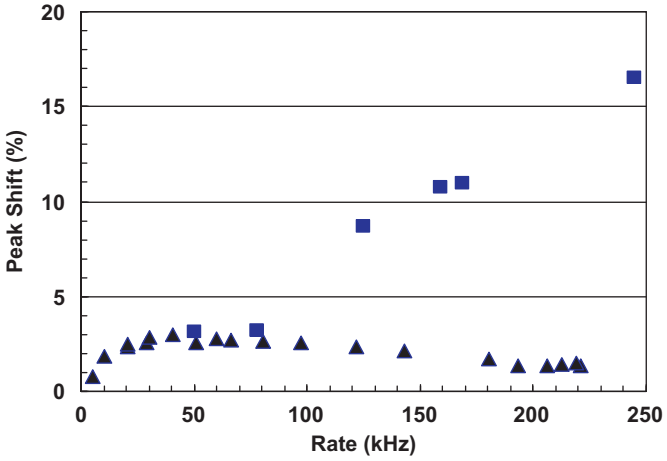

Fig. 4. Measured shift in the peak position as a function of the detector rate as measured with the V1720 digitizer. Squares are relative to the ^{137}Cs gamma ray (0.662 MeV) whereas triangles are related to the shift measured with pulser.

Looking at Fig. 1 in more detail, it appears that the peaks shift at higher energy with increasing the detector rate. This effect appears as well in measurements with standard NIM electronics (7% shift at 20 kHz with respect to the peak position measured at 1 kHz), and does not depend on the gamma ray energy. The shift is magnified at higher rates in the measurements performed with the V1720 digitizer, as illustrated in Fig. 4, with a measured shift value of about 16% at 250 kHz. Also in this case one can learn something from the pulser run: the variation of the pulser peak position up to 220 kHz is generally lower than 3% compared to the 1 kHz value. It is worth noting in Fig. 4 that the shift measured with the pulser is very close to the gamma source values up to 80 kHz and remains constant up to over 200 kHz, whereas the shift of the gamma ray peak position increases remarkably for rates higher than about 80 kHz.

It is quite interesting to notice that the shift in the peak position for rates higher than 80 kHz is clearly associated with the degradation of the energy resolution from about $\delta E/E=2.9\%$ (FWHM) at 80 kHz to about $\delta E/E=3.2\%$ (FWHM) at 220 kHz for the 662 keV ^{137}Cs gamma ray. It is know that the LaBr(Ce) crystal exhibits a significant afterglow component that might affect the signal-to-noise ratio [13] and indeed an interesting correlation of the intrinsic energy resolution of scintillation crystals with their

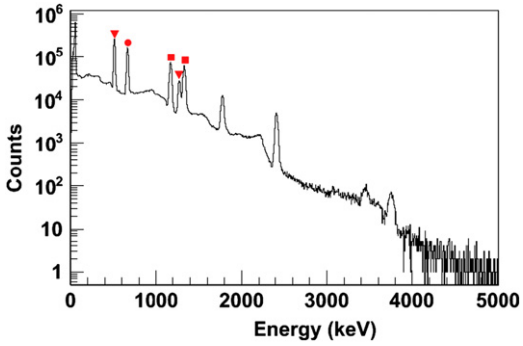

Fig. 5. Gamma ray spectrum taken with a cocktail source at the total rate of 340 kHz. For details see the text. Triangles mark the ^{22}Na (511 and 1275 keV) transitions, the full dot marks the ^{137}Cs transition (662 keV) and the squares mark the ^{60}Co (1.17 and 1.33 MeV) transitions.

afterglow has been recently reported [14]. Thus the shift effect evidenced in Fig. 4 can be qualitatively explained by the afterglow emission in the crystal.

The gamma ray spectrum measured at 340 kHz is presented in Fig. 5. The spectrum was calibrated using ^{241}Am (59 keV), ^{22}Na (511 and 1275 keV), ^{137}Cs (662 keV) and ^{60}Co (1.17 and 1.33 MeV) transitions. It appears that the sum peak of the ^{60}Co source (2.5 MeV) and the 4.4 MeV line from AmBe show up at lower energies than expected, revealing a non-linearity of the system for the largest pulse heights. Such effect has been evidenced in Refs. [9,10] and explained as due to saturations of the PMT. In particular, hardware solutions to this problem have been tested in [10]. As for our detector, this non-linearity has been compensated by using an additional quadratic term into the energy calibration. This procedure is necessary in active interrogations when photons in the range 2–7 MeV are of primary interest.

4. Time resolution results

Timing properties of the experimental setup are important in our application when the system is used in active interrogation with tagged neutron beams. In this case the associated alpha particle, emitted in the final state of the $D+T$ reaction, is detected inside the neutron generator providing the emission time of the neutron and its flight direction, as defined by kinematics. The angular acceptance of the alpha particle detector determines the tagged neutron beam spot at a given distance. The detection time of the neutron induced gamma rays allows one to determine the travel time of the neutron. In this way the time resolution of the system defines the depth of the voxel investigated by the neutron beam [3] which, together with the geometry of the beam spot, provides the definition of the inspected volume.

One of the appealing characteristics of the LaBr(Ce) scintillator is the fast signal with a primary decay time of 16 ns which allows sub-nanosecond resolution.

In this work the time resolution of our LaBr(Ce) detector has been measured by collecting gamma–gamma coincidences, from a ^{22}Na source, against an EJ228 fast plastic detector coupled to an XP2020 PMT.

The shape of the digitized signal for the 662 keV full energy peak in the LaBr(Ce) spectrum measured with the V1720 digitizer is shown in Fig. 6 compared to the signal measured with a Tektronix Digital Oscilloscope (TDS2014B 100 MHz, 1 GS/s). The Digital Oscilloscope signal is obtained as the average of 128 pulses above the trigger level. A typical waveform for the fast plastic is also reported in Fig. 6 derived as an average pulse close to the Compton Edge of the 662 keV transition.

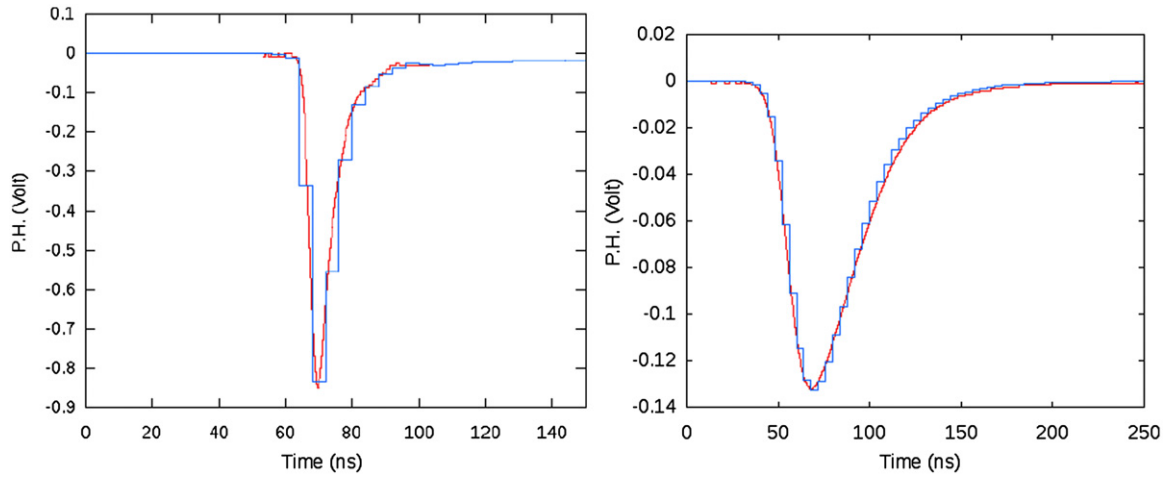

Fig. 6. Histogram of the pulse height versus time of the LaBr(Ce) detector (right panel) and EJ228 plastic scintillator (left panel) measured with the V1720 digitizer. The continuous line is the result of a measure with a Tektronix Digital Oscilloscope. For details see the text.

The rise time of the signals, taken as 10–90% of the signal minimum, is 3.6 ns and 17 ns as measured with the digital oscilloscope for the EJ228 and the LaBr(Ce) detectors, respectively. This reflects in 1 or 2 digitizer bins (1.8 as average value) for the EJ228 and between 4 and 5 digitizer bins (4.2 as average value) for the LaBr(Ce).

The best time resolution of about $\delta t = 0.65$ ns (FWHM) was obtained by processing the LaBr(Ce) and EJ228 PMT anode signals with an ORTEC 935 NIM Constant Fraction Timing Discriminator (CFTD) operated with an external delay of 16 ns for LaBr(Ce) and 3 ns for EJ228. Both detectors were used with low energy thresholds. In any case, a time resolution $\delta t < 0.8$ ns (FWHM) is obtained by varying the CFTD delay in the range 14–18 ns for the LaBr(Ce) detector. The measured time resolution turned out to be rather poor compared to the values reported in Refs. [15–17] for smaller crystals coupled to faster PMTs.

When the anode signals are processed by the V1720 card, the FPGA provides a time stamp for the events in the two detectors. Off-line software analyzes the event file reconstructing the coincidences and the time correlation between detectors. Since in this case the width of each time bin of the digitizer is 4 ns, the achievable time resolution is relatively poor, about $\delta t = 6$ ns (FWHM), when looking directly at the time stamps difference. Better results can be obtained by storing part of the digitized signal for off-line analysis. Several types of software algorithms have been tested (see Ref. [1]).Finally, we have implemented a virtual Constant Fraction Timing Discriminator as described in Ref. [18]. As in common CFTD circuitry, each signal is split: one signal is delayed by a quantity D and the other is inverted and attenuated using the fraction F. Finally the two signals are summed, originating a bipolar signal that provides the timing information at the zero crossing point. In Fig. 7, the virtual CFTD signal is shown for a LaBr(Ce) pulse. In our process the zero crossing value is determined by linear interpolation between the two data points close to the zero baseline.

In order to study the time performance of LaBr(Ce) one has to know the contribution of the fast EJ228 plastic when operated with the digitizer. Consequently a preliminary work was performed on such detectors operated with very low thresholds (about 50 keV on gamma rays). We started using first a single EJ228 detector splitting the signal in two sections of the V1720 digitizer to extract an estimate of the electronic contribution. In this case a resolution as low as $\delta t = 40$ ps (FWHM)was measured. However, a problem was evidenced due to the fact that the EJ228 signal is so fast that it occurs in only few digitizer bins. This

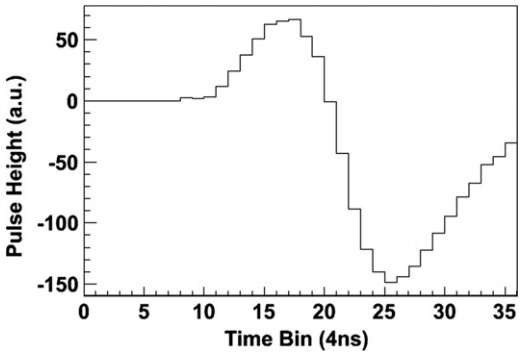

Fig. 7. Computed virtual CFTD signal for a LaBr(Ce) pulse.

produces some instabilities in the analysis with the virtual Constant Fraction when the coincidences between two EJ228 detectors are recorded, depending on the combination of the rise time bins in the two detectors. Such effect disappears for detectors with larger rise-time as the LaBr(Ce) or selecting in the data analysis signals with a rise time characterized by a fixed number of time bins. In any case, the contribution of a single EJ228 detector to the measured time resolution is lower than $\delta t = 0.15$ ns (FWHM). This time resolution value is obtained by using delays $D = 1$ bin (i.e. 4 ns) and fraction of $F = 0.1$. The parameters used in the virtual CFTD have to be compared with those of the ORTEC 935 NIM module. In the latter case the fraction F is fixed at the value $F = 0.2$ and the best results were obtained by using $D = 3$ ns [19]. Consequently the parameters for the hardware and software CFTD are fairly comparable.

Thus the time resolution was studied using one EJ228 fast plastic and the LaBr(Ce) detector. A typical time spectrum is shown in Fig. 8. In this case only signals with a rise time in 1 time bin were selected in the EJ228 plastic.

The time resolution was optimized by searching for the delay D and fraction F parameters for the virtual LaBr(Ce) CFTD. Results from measurements with $F = 0.2$ and 0.4 by varying the delay D are reported in Fig. 9. For $F = 0.2$, as used in the ORTEC 935, the best time resolution is obtained with a quite large delay $D = 10$ bins (i.e. 40 ns). Better results are obtained with $F = 0.4$ for which the optimum resolution corresponds to $D = 7$ bins, i.e. 28 ns. With optimized parameters, the overall time resolution is $\delta t = 0.79$ ns (FWHM) with very low (about 50 keV) threshold and better resolutions are measured by increasing the LaBr(Ce) low energy

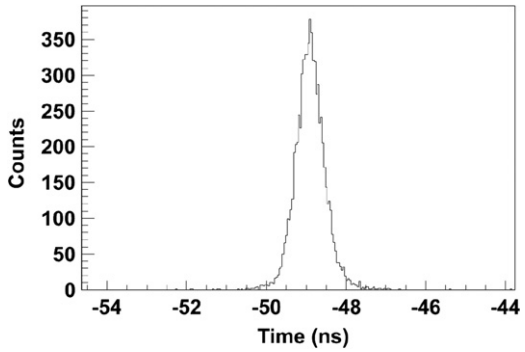

Fig. 8. Example of time spectrum (time difference) between the EJ228 fast plastic and the LaBr(Ce) scintillator.

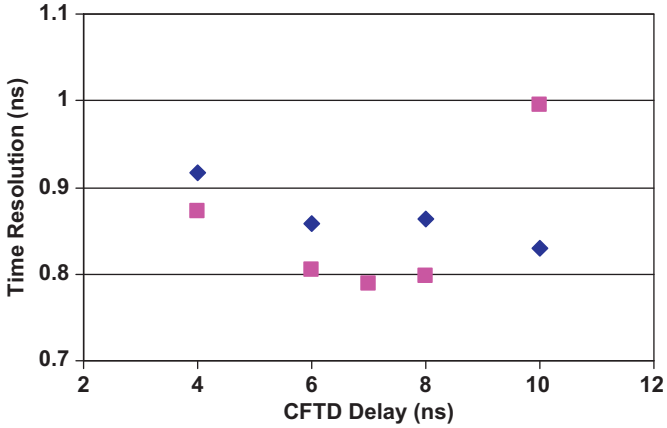

Fig. 9. Measured time resolution (FWHM) by varying the LaBr(Ce) delay D in the virtual CFT: diamonds fraction $F=0.2$, squares fraction $F=0.4$. For details see the text.

Table 2
Summary of time resolution values measured with the V1720 digitizer and with NIM electronics. For details see the text.

Source	LaBr(Ce) threshold (MeV)	Time resolution (FWHM) V1720 (ns)	Time resolution (FWHM) NIM (ns)
^{22}Na	0.05	$\delta t=0.79$	$\delta t=0.65$
^{22}Na	0.50	$\delta t=0.70$	$\delta t=0.53$
^{60}Co	1.0	$\delta t=0.53$	$\delta t=0.47$

thresholds as reported in Table 2. In all the above measurements the EJ228 threshold was always set at about 50 keV. It is worth mentioning that the time resolution from the V1720 remains slightly worse than the one measured with NIM electronics, as documented in Table 2. Finally, the time resolution was studied as a function of the LaBr(Ce) counting rate by varying the detector-to-source distance. Results reported in Fig. 10 show a worsening of the time resolution with increasing rate up to about 100 kHz, being in any case below $\delta t=1.1$ ns (FWHM).

In summary, the time resolution obtained with the V1720 card with the simple virtual CFTD seems to be slightly worse compared to that achieved by using NIM CFTD with hardware compensation for amplitude and rise time. This is certainly due to the relatively small number of time bins used in digitizing the signals and, consequently, in managing our virtual CFTD. In our opinion better results might be obtained by interpolating the zero crossing region with a polynomial function and making use of faster

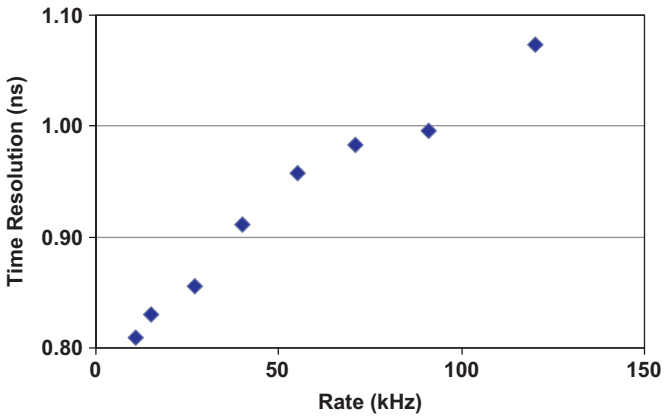

Fig. 10. Measured time resolution (FWHM) as a function of the LaBr(Ce) detector rate.

digitizers. However this would be paid in terms of computing time needed to process the data sets. We would also like to stress upon the fact that the time resolution obtained in this study is sufficiently good for the present application: that is, $\delta t=0.8$ ns (FWHM) reflects in about 4 cm depth for the inspected voxel for 14 MeV tagged neutrons. Voxel depths of the order of 10 cm are a normal choice to assure the required statistical accuracy in the gamma ray spectra compatible with acceptable inspection times [20].

5. Summary and conclusions

The energy resolution of a LaBr(Ce) scintillation detector has been studied as a function of the count rate up to 340 kHz by using a 12 bit 250 MS/s V1720 digitizer. The results for energy resolution are better than those obtained with the same detector equipped with standard NIM shaping amplifiers up to 20 kHz.

Moreover the time resolution achieved by processing off line the digitized signals with a virtual CFTD in a gamma–gamma experiment against a fast plastic scintillator is about $\delta t=0.80$ ns (FWHM) slightly worse compared to $\delta t=0.65$ ns (FWHM) obtained when standard NIM CFTDs are used. However, the time resolution obtained with the V1720 digitizer is more than adequate for applications in Non-Destructive Analysis of large objects with tagged neutron beams.

References

[1] D. Cester, et al., Nuclear Instruments and Methods A 663 (2012) 55–63.
[2] see ⟨http://www.elsagdatamat.com/PDF/EDLink34.pdf⟩.
[3] S. Pesente, et al., Nuclear Instruments and Methods B241 (2005) 743.
[4] P.R. Menge, et al., Nuclear Instruments and Methods A579 (2007) 6–10 and references therein.
[5] S. Kurosawa, et al., Nuclear Instruments and Methods A623 (2011) 249.
[6] R. Scafè, et al., Nuclear Instruments and Methods A643 (2011) 89.
[7] More Technical Details are Reported in the V1720 USER MANUAL. Available from: ⟨www.caen.it⟩.
[8] More Technical Details are Reported in the DPP_CI_runner-User Manual. Available from: ⟨www.caen.it⟩.
[9] M. Ciemala, et al., Nuclear Instruments and Methods A608 (2009) 76.
[10] F.G.A. Quarati, et al., Nuclear Instruments and Methods A629 (2011) 157.
[11] E.K. Mace, L.E. Smith, Nuclear Instruments and Methods A652 (2011) 62.
[12] Rita C. Pereira, et al., IEEE Transactions on Nuclear Science NS-58 (2011) 1531.
[13] Douraghy Ali, et al., Nuclear Instruments and Methods A569 (2006) 557.
[14] M. Moszynski, Radiation Measurements 45 (2010) 372.
[15] R. Nicolini, et al., Nuclear Instruments and Methods A582 (2007) 554.
[16] D. Weisshaar, et al., Nuclear Instruments and Methods A594 (2008) 56.
[17] S. Zhu, et al., Nuclear Instruments and Methods A652 (2011) 231.
[18] A. Fallu-Labruyere, et al., Nuclear Instruments and Methods A579 (2007) 247.
[19] L. Stevanato, Thesis, University of Padova, 2009, unpublished.
[20] C. Carasco, et al., Nuclear Instruments and Methods A588 (2008) 40.